Comparing Five Kinematic Wave Schemes for Open-Channel Routing for Wide-Tooth-Comb-Wave Hydrographs

Charles Luo, Ph.D., P.Eng.[1]

Abstract: Due to its simplicity, the kinematic wave is commonly applied to open-channel routing in watershed hydrologic modeling. However, these applications must fulfill certain conditions, such as relatively large riverbed slopes and long time of rise in the flow. This study attempts to determine the most appropriate kinematic wave scheme for open-channel routing in the highly regulated Peace River, Canada. Five schemes were used to simulate a 5-day hydrograph with sudden plunges and hikes. The outputs from these five schemes were compared visually and statistically with the observed hydrograph. It was found that all five schemes are applicable to open-channel routing for the highly regulated Peace River if the temporal and spatial increments are set properly. However, one scheme, which is a total variation diminishing (TVD) high-resolution scheme, is the most appropriate scheme for this purpose. This scheme allows large temporal and spatial increments while relatively high accuracy can be achieved. **DOI: 10.1061/(ASCE)HE.1943-5584.0002079.**

Author keywords: Kinematic wave; Open-channel routing; High-resolution scheme; Total variation diminishing (TVD).

Introduction

British Columbia is the third largest province in Canada and the total area is about 947,900 km^2. Floods are the most damaging natural hazards in British Columbia (Foster 2001). Thus, timely real-time flood forecasts and flood warnings covering the entire province are critical for British Columbia communities. However, flood forecasting tasks, which involve a hydrologic model, could be overwhelming and face great difficulties because of the immense heterogeneity in such a large area. One of the core elements of a hydrologic model is the open-channel routing. In the real-time flood forecasting in British Columbia, one of the greatest difficulties facing the modelers may be the routing of flows with sudden plunges and hikes, or the so-called wide-tooth-comb-wave hydrographs, in the 150-km reach of the highly regulated Peace River. To the best of the author's knowledge, there is no previous published work that explicitly tackles this issue. At this stage, the objective of this study is to select an appropriate numerical scheme for the open-channel routing for the wide-tooth-comb-wave hydrographs. An appropriate numerical scheme should be a time-efficient scheme that allows the use of relatively large temporal and spatial increments while relatively high modeling accuracy may still be achieved.

From the perspective of modeling accuracy, the numerical solution of the full Saint-Venant equations, or the dynamic wave routing, could be the first selection. However, for complicated river networks, this routing becomes inefficient for real-time flood operation because of formidable computational requirements and large error accumulations (Tsai 2003). Moreover, a more complex model requires more parameters to be estimated and more field data to be measured (Tsai 2003). In this study, the modeled reach in the Peace River is about 150 km long, and the final goal of this study is to apply the selected numerical scheme to most of the rivers in British Columbia, which have a total length of 42,125 km. For such a large river length, it is very difficult, if not completely impossible, to obtain all the necessary field survey data for the modeling. Based on this consideration and the findings by Tsai (2003), dynamic wave or diffusive wave routing is not a choice in this study.

On the other hand, due to its simplicity, the kinematic wave is commonly adopted for open-channel routing in watershed hydrologic modeling, especially for time-sensitive real-time flood forecasting in large-scale watersheds. One advantage of kinematic wave routing is that it can be developed with little or no streamflow data (Dawdy 1990). After comparing the hydrographs from numerical solutions of the kinematic wave and those from outputs of the dynamic wave, Lee and Huang (2012) concluded that the deviation of the hydrographs from the two numerical solutions is small enough if the channel slope is larger than 0.001. Ponce (1996) defined a broadened criterion for the applicability of the kinematic wave and stated that the kinematic wave is applicable for a wide range of field situations, both short mountain streams and long alluvial rivers, both steep and mild basins, and both fast-rising and slow-rising hydrographs, provided that the product of the time to peak (or time of rise) and the riverbed slope is significantly large.

However, applying the kinematic wave open-channel routing to the hydrologic modeling in the large-scale watersheds in British Columbia may also face many challenges. One of these challenges is the requirement of routing the wide-tooth-comb-wave hydrographs observed in the highly regulated Peace River. The riverbed slope in the lower reach of the Peace River flowing through the flat prairie within the British Columbia boundary is usually smaller than 0.001. Because the river is highly regulated, some of the observed hydrographs may include sudden plunges and hikes, which result in a very short time of rise, sometimes as short as 3 h. The product of this small riverbed slope of the lower reach of the Peace River and the short time of rise of the wide-tooth-comb-wave hydrographs may not fulfill Ponce's (1996) criterion.

[1]BC River Forecast Centre, 2975 Jutland Rd., Victoria, BC, Canada V8T 5J9. ORCID: https://orcid.org/0000-0002-9265-4698. Email: Charles.Luo@gov.bc.ca

Note. This manuscript was submitted on March 13, 2019; approved on December 21, 2020; published online on February 9, 2021. Discussion period open until July 9, 2021; separate discussions must be submitted for individual papers. This paper is part of the ***Journal of Hydrologic Engineering***, © ASCE, ISSN 1084-0699.

In this study, in order to examine the applicability of the kinematic wave to the open-channel routing for the wide-tooth-comb-wave hydrographs observed in the 150-km-long highly regulated Peace River, five kinematic wave schemes were used to route the 5-day wide-tooth-comb-wave hydrograph observed in the Peace River from February 12 to 16, 2016. Because the time step for the Channel Link Evolution Efficient Routing (CLEVER) model for real-time flood forecasting in British Columbia is 1 h (3,600 s) (Luo 2015), seven basic scenarios with an hourly time step were designed for the five schemes to simulate the 5-day wide-tooth-comb-wave hydrograph. In order to further examine the sensitivity of the five schemes to the temporal increment, seven extended scenarios with a 5-min time step were also designed for the five schemes to route the first 35 h of the 5-day wide-tooth-comb-wave hydrograph. Details of the scenarios are given in the "Results" section.

In the next sections, the regulated reach of the Peace River is described, and then five kinematic wave schemes, four commonly used and one developed for real-time flood forecasting in British Columbia, are related. After that, the results from these five schemes for seven basic scenarios and seven extended scenarios are analyzed and evaluated visually and statistically.

Regulated Peace River

The Peace River, which originates in the northern British Columbia part of the Rocky Mountains and flows to the northeast through the prairie into Alberta, Canada, is the third largest river in British Columbia with respect to its watershed area within the British Columbia boundary (123,671 m^2). The river is regulated by the W. A. C. Bennett Dam and the Peace Canyon Dam, both of which control the downstream flow of the Peace River through human operation of the gates and spillways of the dams. About 8.5 km downstream from the Peace Canyon Dam (hereinafter referred to as the dam), there is a Water Survey of Canada (WSC) station, the Peace River at Hudson Hope (07EF001), which records the regulated discharge from the dam plus the very small amount of natural inflows from the tiny local drainage area (385 km^2) between the dam and the station. About 150 km downstream, there is another WSC station, the Peace River above Alces River (07FD010). The average slope (S_0) between these two WSC stations is 0.000743. In the river reach between these two stations, there are two other WSC stations located in the Peace River and five more WSC stations located in the outlets of five major tributaries, which are, from upstream to downstream, the Halfway River, the Moberly River, the Pine River, the Beatton River, and the Kiskatinaw River. Fig. 1 is a GIS map of the highly regulated reach of the Peace River and its major tributaries between the dam and the downstream WSC station Peace River above Alces River (07FD010).

The WSC station Peace River at Hudson Hope (07EF001) recorded a very interesting, wide-tooth-comb-wave hydrograph in the beginning of each of the recent year's freshet season, from middle February to early June. This reflected the human operation of the gates and spillways of the dam. Fig. 2 shows a 5-day (from February 12 to 16, 2016) hydrograph of this kind. The hydrograph in Fig. 2 plunges and hikes by 1,250 m^3/s in about 3 h. This means that the time of rise is only about 3 h. This human-produced discharge pattern, which flows in the natural river system and converges with the inflows from the tributaries, poses a big challenge to open-channel routing. However, this also provides a rare opportunity to evaluate the efficiency and capability of different numerical schemes for the kinematic wave. In this study, the wide-tooth-comb-wave hydrograph recorded at the WSC station Peace River at Hudson Hope (07EF001) from February 12 to 16, 2016 was used as the input hydrograph for open-channel routing.

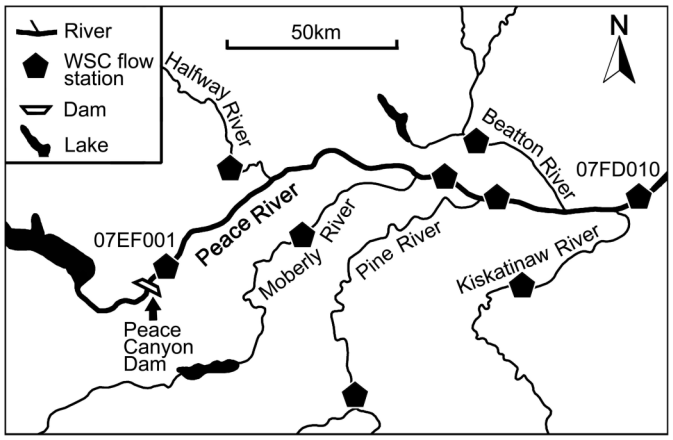

Fig. 1. Highly regulated reach of Peace River between Peace Canyon Dam and WSC station 07FD010 (56°07′36″ N, 120°03′26″ W). (Map created by author.)

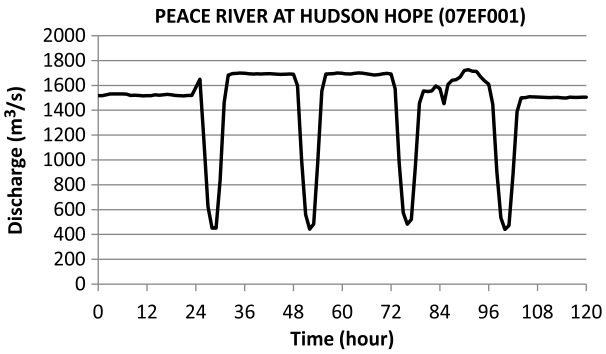

Fig. 2. Five-day (from February 12 to 16, 2016) wide-tooth-comb-wave hydrograph recorded at station 07EF001.

It was found that from February 12 to 16, 2016, all the tributaries between the upstream station (07EF001) and downstream station (07FD010) flowed at their base flows and the total inflow from these tributaries was 33 m^3/s, which was only 2.2% of the average flow recorded at the downstream station (07FD010) for this period of the year. The local drainage area that is not controlled by the WSC stations of the tributaries between the upstream station (07EF001) and downstream station (07FD010) in the Peace River is 6,240 km^2, which is only 5.2% of the total drainage area (121,000 km^2) of the downstream station (07FD010). The lateral inflow from this local drainage area was negligible because the snowmelt season had not started yet in this period of the year.

Methodology

Four Commonly Used Numerical Schemes for Kinematic Wave Open-Channel Routing

Chow et al. (1988) presented two first-order numerical schemes, the linear scheme and nonlinear scheme, which have been largely used in watershed modeling. It was found that the results from both the Chow linear and nonlinear schemes are very similar (Chow et al. 1988) and thus the Chow linear scheme was used for comparison in

Table 1. Summary of four commonly used kinematic wave schemes for open-channel routing

Scheme	Source	Discretizing method	Advantages	Known limitations
Chow linear	Chow et al. (1988, pp. 294–302)	Backward difference	Simple and short computation time	Degree of dispersion increasing with size of Δx and Δt (p. 300)
HEC	USACE (2000)	Leclerc and Schaake	Stable	Spatial and temporal steps varying with flow depths and time of rise
KINEROS	Smith et al. (2012)	Four-point implicit method	High resolution	Intrinsically unstable for certain cases
MC	Fread (1993)	Linear correlation	Simple, less wave attenuation	Lack of mass balance, not for routing flows with rise time less than 2 h

this study. Another commonly used first-order scheme is the Hydrologic Engineering Center (HEC) scheme, which includes HEC-1 (USACE 1993) and the Hydrologic Modeling System (HEC-HMS) (USACE 2000). The HEC scheme is deliberately designed to avoid the unstable issue by switching between the standard form and conservation form. In the HEC model, the standard form is used when the stability factor is less than 1 or the kinematic wave celerity (c_k) is smaller than the quotient of the spatial increment and the temporal increment ($\Delta x/\Delta t$), and the conservation form is used otherwise. In the meantime, the Kinematic Simulation of Catchment Runoff and Erosion Processes (KINEROS) (Smith et al. 2012), which was developed at the Southwest Watershed Research Center of the United States Department of Agriculture, is another commonly used scheme for kinematic wave open-channel routing. The KINEROS scheme is actually a second-order scheme, which is intrinsically unstable for certain types of hydrographs and certain sizes of spatial and temporal increments even though a weighting factor ($\theta = 0.6$–0.8) is introduced to the space derivative (only) (Smith et al. 2012; Preissmann 1961). In addition to these three schemes, the Muskingum-Cunge (MC) approach, as a variation of the standard kinematic wave method, is also commonly used for open-channel routing in the hydrologic community (Fread 1993; Todini 2007). Equations of these four schemes are available from easily accessible references and therefore are omitted here for conciseness of this paper. Table 1 summarizes these four commonly used kinematic wave schemes with respect to their sources, discretizing methods, advantages, and known limitations.

These four numerical schemes were commonly used for operational kinematic wave open-channel routing in the US and other countries. Other schemes, such as the Godunov-type schemes, which are more effective for the discontinuous overland flow routing (Godunov 1959), may be included in future studies.

CLEVER Model Scheme

The CLEVER model (Luo 2015; Luo et al. 2015) is a hybrid watershed model that was developed for operational real-time flood forecasting for the large-scale, snowmelt-dominated watersheds in British Columbia. The CLEVER model consists of a lumped watershed routing submodel and a distributed open-channel routing submodel that adopts the kinematic wave simplification for the Saint-Venant equations. In the kinematic wave simplification, the inertial and pressure terms in the momentum equation are neglected, and it is assumed that the flow is steady and uniform and that the friction slope is equal to the slope of the channel (Chow et al. 1988). The kinematic wave equations are given as follows when there is no lateral inflow:

$$\frac{\partial Q}{\partial x} + \frac{\partial A}{\partial t} = 0$$
$$S_0 = \frac{n^2 Q^2}{A^2 R^{4/3}} \tag{1}$$

in which Q = discharge; x and t = spatial and temporal coordinates, respectively; A = cross-section area; S_0 = channel slope; n = Manning's roughness coefficient; and R = hydraulic radius and is calculated with $R = A/P$, where P is the wet perimeter.

In this study, a finite-difference scheme similar to the Preissmann (1961) scheme was adopted to discretize the continuity equation of the kinematic wave by setting both of the Preissmann spatial and temporal weighting coefficients to 0.5. Discretizing the continuity equation and after some rearrangements, the implicit equation is derived from Eq. (1)

$$A_{i,j} = \frac{\Delta t(Q_{i-1,j} + Q_{i-1,j-1} - Q_{i,j-1}) + \Delta x(A_{i,j-1} + A_{i-1,j-1} - A_{i-1,j})}{\Delta t V_{i,j} + \Delta x} \tag{2}$$

in which i and j = spatial and temporal steps on the x- and y-coordinates, respectively; (i, j) = unknown node; Δx and Δt = spatial and temporal increments, respectively; and

$$V_{i,j} = \frac{1}{n}\sqrt{S_0} R_{i,j}^{2/3} \tag{3}$$

If $A_{i,j}$ and $V_{i,j}$ are solved, $Q_{i,j}$ can be found

$$Q_{i,j} = V_{i,j} A_{i,j} \tag{4}$$

However, Eq. (2) is unsolvable because $V_{i,j}$ is also an unknown. In order to solve Eq. (2), the Semi-Implicit Method for Pressure-Linked Equations (SIMPLE) (Patankar and Spalding 1972) is introduced. Pressure is a concept in fluid dynamics and the relevant concept in hydrology is water head or water depth (Luo 2007). The iteration method in Luo (2007) is adopted to solve Eq. (2) iteratively

$$(A_{i,j})^{(k)} = \frac{\Delta t(Q_{i-1,j} + Q_{i-1,j-1} - Q_{i,j-1}) + \Delta x(A_{i,j-1} + A_{i-1,j-1} - A_{i-1,j})}{\Delta t (V_{i,j})^{(k-1)} + \Delta x} \tag{5}$$

in which $(k-1)$ and (k) = iteration steps.

The Preissmann (1961) scheme is a second-order scheme and thus Eq. (5) is not a total variation diminishing (TVD) or oscillation free for the kinematic wave routing. In order to obtain a TVD solution, a nonnegative flux limiter $\varphi(r)$ (r is the ratio of the consecutive gradients or the smoothness parameter) (Sweby 1984) is applied to the antidiffusive flux term in Eq. (5) and the equation becomes

$$(A_{i,j})^{(k)} = \frac{\Delta t Q_{i-1,j} + \Delta x A_{i,j-1}}{\Delta t (V_{i,j})^{(k-1)} + \Delta x} + \varphi(r_{ij}) \frac{\Delta t (Q_{i-1,j-1} - Q_{i,j-1}) + \Delta x (A_{i-1,j-1} - A_{i-1,j})}{\Delta t (V_{i,j})^{(k-1)} + \Delta x} \quad (6)$$

Because the CLEVER model was developed for real-time flood forecasting in the large-scale watersheds in British Columbia, uniform initial conditions are applied to the open channel and coarse spatial increments are preferable to achieve time efficiency or short computation time. For the same reason, in some of the watersheds, the number of channel segments may be as few as two. Therefore, the ratio of consecutive gradients (r) is not defined along the spatial axis, but rather on the temporal axis and given by

$$r_{i,j} = \frac{Q_{i-1,j-1} - Q_{i-1,j-2}}{Q_{i-1,j} - Q_{i-1,j-1}} \quad (7)$$

Nine second-order TVD flux limiters were studied and compared in the CLEVER model. These limiters are (1) Minmod (Roe 1981), (2) Superbee (Roe 1986), (3) Van Leer (1974), (4) Osher (Chakravarthy and Osher 1983), (5) Van Albada et al. (1982), (6) Sweby (1984), (7) Ospre (Waterson and Deconinck 1995), (8) Monotonized Central (Van Leer 1977), and (9) Umist (Lien and Leschziner 1994). As the result of the comparison, the Minmod (Roe 1981) limiter was selected for Eq. (6) and is given by

$$\varphi(r) = \max[0, \min(1, r)] \quad (8)$$

Statistical Indicators for Evaluation of Results

In order to obtain a more objective judgment, a number of statistical indicators were employed to evaluate the goodness of fit of the simulated hydrograph to the observed one. These statistical indicators include (1) the coefficient of model efficiency (Ce), which describes how well the volume and timing of the simulated hydrograph compares to the observed hydrograph, with a value closer to 1 indicating a better fit of the simulated hydrograph to the observed hydrograph (Nash and Sutcliffe 1970), (2) the coefficient of model determination (Cd), which measures how well the shape of the simulated hydrograph reflects the observed hydrograph and depends solely on the timing of changes in the hydrograph, with a value closer to 1 indicating a better fit of the simulated hydrograph to the observed hydrograph (Nash and Sutcliffe 1970), (3) the percentage volume difference (dV) of the simulated hydrograph relative to the observed hydrograph (Nash and Sutcliffe 1970), and (4) the relative mean absolute error (Era) of the simulated hydrograph to the observed hydrograph (Lettenmaier and Wood 1993).

Results

Model Input, Parameters, and Initial and Boundary Conditions

In this study, the Chow linear, HEC, KINEROS, MC, and CLEVER schemes were used to separately route the regulated, wide-tooth-comb-wave hydrograph recorded at the upstream station (07EF001) as given in Fig. 2 to the downstream station (07FD010). The discharge recorded at the upstream station (07EF001) was the input to the five schemes and discharge recorded at the downstream station (07FD010) was used to calibrate and verify the output hydrographs from these five numerical schemes.

Table 2. Basic scenarios

River length (km)	Δx (km)	Δt (s)	$\Delta x/\Delta t$ (m/s)	River segments	Scenario
150	1	3,600	0.278	150	SCN1
150	2.5	3,600	0.694	60	SCN2
150	5	3,600	1.389	30	SCN3
150	7.5	3,600	2.083	20	SCN4
150	10	3,600	2.778	15	SCN5
150	25	3,600	6.944	6	SCN6
150	50	3,600	13.889	3	SCN7

Note: $\Delta t = 1$ h $= 3{,}600$ s.

The channel was assumed to be rectangular with the following parameters: width (b) = 100 m and slope (S_0) = 0.000743. The Manning's roughness coefficient (n) was subject to calibration. Theoretically, the smaller the temporal and spatial increments a numerical scheme adopts, the higher accuracy its solution has. Scenario SCN1, which is defined in Table 2, has the smallest spatial increment (1 km) among the seven scenarios and the same temporal increment (1 h) as the other scenarios. In order to reduce the bias in the comparison of simulation results from the five numerical schemes so that they are comparable, the Manning's roughness coefficient (n) was calibrated separately with Scenario SCN1 for each of the five schemes to such an extent that the simulated hydrograph matched the best observed one for this scenario. The calibration results of the Manning's roughness coefficient (n) are 0.078, 0.075, 0.068, 0.078, and 0.062 for Chow linear, HEC, KINEROS, MC, and CLEVER, respectively. These values are within the range of the base values plus the adjustments from the channel's irregularity, variation in cross section, obstructions, vegetation, and meandering. The base values and adjustments can be found in other studies, e.g., Phillips and Tadayon (2007). The simulated discharge is the outflow from each of the five numerical schemes plus the total inflow from all the major tributaries (33 m^3/s) between the upstream and downstream stations. The observed discharge is the flow recorded at the downstream station (07FD010).

The initial conditions include the observed discharge (Q) at the upstream station (07EF001) and the cross-section area (A) at the starting time step ($t = 0$). Both Q and A are uniformly distributed to all spatial grids when $t = 0$. The upstream boundary conditions are the observed time series of Q at the upstream station (07EF001). No downstream boundary conditions are necessary in this study because the finite-difference scheme is explicit from upstream to downstream.

Basic Scenarios

Seven basic scenarios with an hourly time step are defined in Table 2. In order to examine the performances of the five numerical schemes to the full extent, these scenarios were designed so that the quotient of $\Delta x/\Delta t$ covers a wide spectrum from a flow much smaller than the minimum kinematic wave celerity of the inflow (1.731 m/s) to that much larger than the maximum kinematic wave celerity of the inflow (2.77 m/s). All seven basic scenarios routed the 5-day wide-tooth-comb-wave hydrograph from February 12 to 16, 2016, through the 150-km reach of the Peace River.

Visual Comparisons of Simulated and Observed Hydrographs for Basic Scenarios

Figs. 3(a–e) show comparisons of the simulated hydrographs output from the five numerical schemes with the observed flow

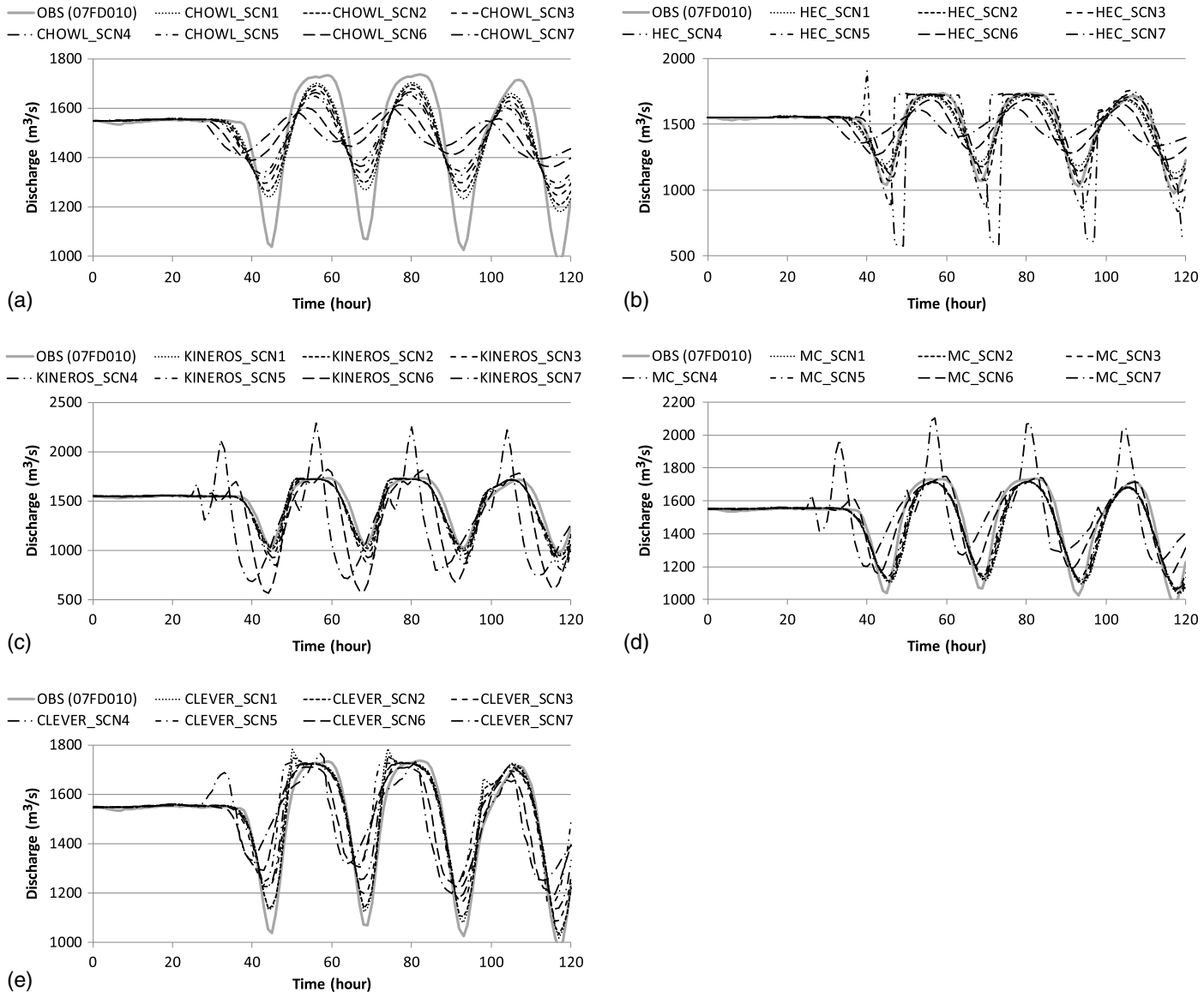

Fig. 3. Comparisons of simulated hydrographs output from five schemes: (a) Chow linear (CHOWL); (b) HEC; (c) KINEROS; (d) MC; and (e) CLEVER, with observed hydrograph for seven basic scenarios.

recorded at the downstream station (07FD010). These comparisons provide a visual basis for the judgment of model calibration and verification. First, Fig. 3 shows that the simulated hydrographs from four of the five schemes (excluding the Chow linear) for certain scenarios, such as SCN1, SCN2, and SCN3, match the observed hydrograph very well. This means that the kinematic wave schemes of the HEC, KINEROS, MC, and CLEVER can be applied to the open-channel routing for rivers with a riverbed slope smaller than 0.001 (equal to 0.000743 in this study) and for the flow with a rising time as short as 3 h if the size of the spatial increment is set properly. Second, Fig. 3 shows that the Chow linear scheme has the largest numerical dispersion for all the basic scenarios among the five schemes and the CLEVER scheme demonstrates smaller numerical dispersion than the Chow linear scheme for all the scenarios. Third, Fig. 3 also shows that the HEC scheme has the largest error for SCN4 and both the KINEROS and MC schemes have oscillations for SCN7, while large errors or oscillations are not present in the CLEVER scheme for any of the seven scenarios.

Statistical Evaluation of Simulation Results for Basic Scenarios

Table 3 lists the statistics for the simulation results from the Chow linear, HEC, KINEROS, MC, and CLEVER schemes for all the basic scenarios. Table 3 shows that the values of *Ce* and *Cd* for the Chow linear scheme for SCN1–SCN3 are acceptable but not as good as those for the other four schemes, and these values decrease substantially from Scenarios SCN1 to SCN5 and become very small for Scenarios SCN6 and SCN7 because large numerical dispersion is present in these scenarios. This feature of the Chow linear scheme is due to its limitations listed in Table 1.

For the HEC scheme, the values of *Ce* and *Cd* are very high for Scenarios SCN1–SCN3, but the value of *Ce* becomes negative for Scenario SCN4 due to the large errors incurred by switching of

Table 3. Statistics of simulation results for basic scenarios

Scheme	Scenario	*Ce*	*Cd*	*dV* (%)	*Era* (%)
Chow linear	SCN1	0.850	0.919	−0.111	3.890
	SCN2	0.804	0.898	0.050	4.425
	SCN3	0.727	0.855	0.242	5.204
	SCN4	0.655	0.805	0.375	5.866
	SCN5	0.588	0.749	0.472	6.413
	SCN6	0.294	0.380	0.741	8.583
	SCN7	0.028	0.038	0.869	10.270
HEC	SCN1	0.906	0.939	−0.338	3.074
(combined standard	SCN2	0.942	0.958	−0.370	2.443
and conservation forms)	SCN3	0.953	0.955	−0.444	1.995
	SCN4	−0.216	0.502	−2.519	6.586
	SCN5	0.694	0.840	0.999	4.208
	SCN6	0.664	0.716	−0.294	5.730
	SCN7	0.176	0.177	−0.229	9.414
KINEROS	SCN1	0.943	0.956	−0.924	2.408
($\theta = 0.7$)	SCN2	0.932	0.958	−1.356	2.716
	SCN3	0.898	0.958	−2.141	3.273
	SCN4	0.837	0.955	−3.032	3.982
	SCN5	0.733	0.950	−4.068	4.823
	SCN6	−0.320	0.846	−8.798	10.445
	SCN7	−2.180	0.228	−9.350	16.736
MC	SCN1	0.87	0.897	−2.321	3.505
	SCN2	0.883	0.906	−2.063	3.367
	SCN3	0.904	0.922	−1.655	3.129
	SCN4	0.923	0.938	−1.274	2.871
	SCN5	0.939	0.954	−0.902	2.591
	SCN6	0.871	0.892	1.047	3.155
	SCN7	0.111	0.335	2.934	10.041
CLEVER	SCN1	0.941	0.955	1.613	2.110
	SCN2	0.955	0.967	1.346	1.997
	SCN3	0.927	0.962	1.656	2.514
	SCN4	0.873	0.926	2.147	3.215
	SCN5	0.671	0.741	3.271	4.867
	SCN6	0.593	0.601	0.864	5.972
	SCN7	0.355	0.365	0.991	7.678

the equations in this scenario. Moreover, the values of *Ce* and *Cd* for the HEC scheme also become very small for Scenario SCN7 because of the large numerical dispersion that is present in the scenario. This could be a consequence of the scheme's discretizing method.

For the KINEROS scheme, the values of *Ce* and *Cd* are good enough for Scenarios SCN1–SCN5. However, the value of *Ce* for the KINEROS scheme becomes negative in both Scenarios SCN6 and SCN7 because of the oscillation and reversed numerical dispersion that is present in these scenarios. The value of *Cd* in Scenario SCN7 also drops to a very small value. The *Era* value in Scenario SCN7 is the largest (worst) (16.7%) among all five schemes in all the basic scenarios. These large errors may have a connection with the scheme's intrinsic unstableness.

For the MC scheme, the statistics shows that the scheme performs best for Scenario SCN5 among the seven basic scenarios and worst for Scenario SCN7 due to the oscillation that is present in this scenario. Unlike the other four schemes, the MC scheme does not perform best for Scenario SCN1, in which the size of the spatial increment is the smallest. This may be because the MC scheme lacks mass balance as pointed out by Todini (2007).

The CLEVER scheme performs very well for Scenarios SCN1–SCN4 and the statistics decrease from Scenarios SCN5 to SCN7. However, the worst scenario (SCN7) of the CLEVER scheme has the best statistics, except for *dV*, among all five schemes. This is because the CLEVER scheme is a TVD scheme.

Table 4. Extended scenarios

River length (km)	Δx (km)	Δt (s)	$\Delta x/\Delta t$ (m/s)	River segments	Scenario
150	0.25	300	0.833	600	SCN11
150	0.50	300	1.667	300	SCN12
150	0.75	300	2.500	200	SCN13
150	1	300	3.333	150	SCN14
150	2.5	300	8.333	60	SCN15
150	5	300	16.667	30	SCN16
150	10	300	33.333	15	SCN17

Note: $\Delta t = 5$ min $= 300$ s.

Extended Scenarios at a 5-min Time Step and Visual and Statistical Evaluation

The essence of the discretizing methods for the five kinematic wave schemes is the finite-difference method, for which, theoretically, the smaller the temporal and spatial increments, the higher the modeling accuracy that may be achieved. The original time step for the observed discharge is 5 min. In order to further examine the performances of the five schemes at a shorter time step, seven extended scenarios with a 5-min time step are defined in Table 4. The criteria for designing the extended scenarios are the same as those for the basic scenarios in the section "Basic Scenarios." All seven extended scenarios routed the first 35 h of the 5-day wide-tooth-comb-wave hydrograph through the 150-km reach of the Peace River.

Figs. 4(a–e) compare the simulated hydrographs output from the five schemes with the observed flow recorded at the downstream station (07FD010) for all seven extended scenarios. The figures only show the results for a shortened time span from 600 min (10 h) to 2,000 min (33.333 h) so that the lines are easier to distinguish. For easier comparisons, all results for the seven extended scenarios from each of the five numerical schemes are plotted together in Figs. 4(a–e). Table 5 lists the statistics for the simulation results from the five schemes for all seven extended scenarios. Comparing Fig. 4 with Fig. 3 and Table 5 with Table 3, it can be seen that, for all five kinematic wave schemes, a smaller temporal increment, with smaller spatial increments, does not necessarily mean higher simulation accuracy.

For the Chow linear scheme, SCN16 has the highest accuracy among all the extended scenarios, which is better than that for all the basic scenarios. Scenarios with smaller spatial increments (SCN11, SCN12, SCN13, and SCN14) have larger errors. For the HEC scheme, the largest error is present in SCN12 and this error is greater than the largest error in the basic scenario SCN4. This largest error is also incurred by switching of the equations in Scenario SCN12. For the KINEROS scheme, the accuracy for SCN11, SCN12, and SCN13 is much lower than that for the relevant basic scenarios. The scheme has no solution for SCN14, SCN15, SCN16, and SCN17 because this is a second-order scheme. Generally speaking, the MC scheme has higher or similar accuracy for all the extended scenarios than that for the basic scenarios. This may be because smaller temporal and spatial increments may also have a better mass balance for the MC scheme. The MC scheme is also the best among the five schemes for all the extended scenarios.

The accuracy of the CLEVER scheme is moderate for all the extended scenarios among the five schemes. Comparing with the other schemes, the CLEVER scheme has no scenario with

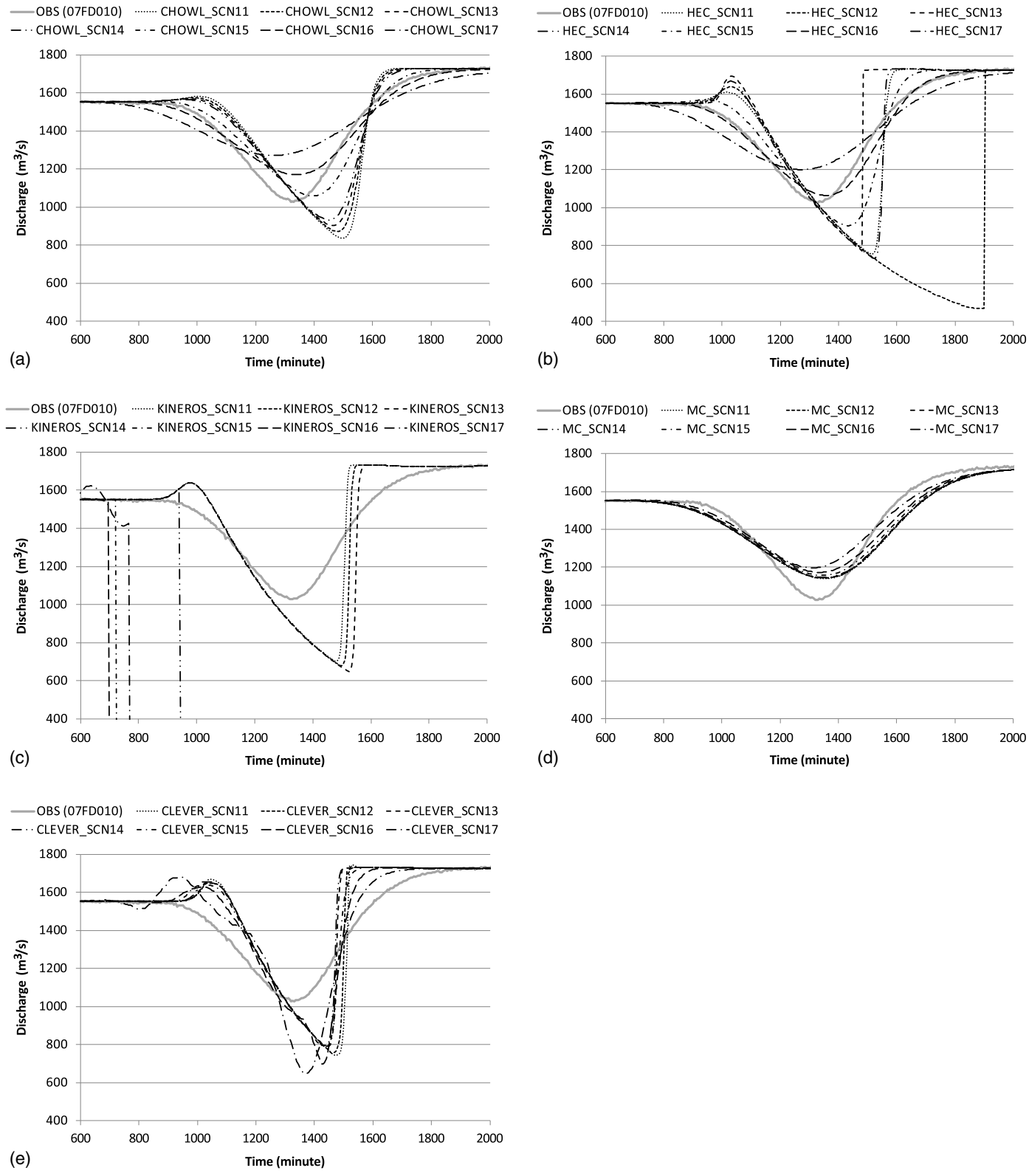

Fig. 4. Comparisons of simulated hydrographs output from five schemes: (a) Chow linear (CHOWL); (b) HEC; (c) KINEROS; (d) MC; and (e) CLEVER, with observed hydrograph for seven extended scenarios.

statistics as bad as the HEC scheme in SCN12, and has no scenario without a solution like the KINEROS scheme does. However, Fig. 4(e) also shows the limitation of the CLEVER scheme. The limitation is that, when the temporal increment is set to as short as 5 min, the CLEVER scheme cannot produce enough numerical dispersion, which is necessary for the open-channel routing for the wide-tooth-comb-wave hydrographs, as the other schemes except for the KINEROS scheme do, by increasing the spatial increment size only. This is a side effect of applying a TVD flux limiter. Due to this limitation, the CLEVER scheme may not be the best scheme

Table 5. Statistics of simulation results for extended scenarios

Scheme	Scenario	*Ce*	*Cd*	*dV* (%)	*Era* (%)
Chow linear	SCN11	0.535	0.711	−0.126	4.337
	SCN12	0.634	0.755	−0.003	3.940
	SCN13	0.711	0.793	0.084	3.579
	SCN14	0.772	0.826	0.152	3.248
	SCN15	0.942	0.943	0.377	1.784
	SCN16	0.950	0.976	0.532	1.574
	SCN17	0.807	0.886	0.657	3.369
HEC (combined standard and conservation forms)	SCN11	0.436	0.711	−0.210	4.606
	SCN12	−5.390	0.019	−13.146	16.282
	SCN13	0.534	0.723	2.045	4.581
	SCN14	0.357	0.692	−0.201	4.883
	SCN15	0.814	0.884	−0.210	2.814
	SCN16	0.983	0.983	−0.213	0.946
	SCN17	0.885	0.912	−0.218	2.776
KINEROS ($\theta = 0.7$)	SCN11	0.487	0.818	−0.455	4.390
	SCN12	0.387	0.801	−1.088	4.624
	SCN13	0.207	0.764	−1.953	5.038
	SCN14	N/S	N/S	N/S	N/S
	SCN15	N/S	N/S	N/S	N/S
	SCN16	N/S	N/S	N/S	N/S
	SCN17	N/S	N/S	N/S	N/S
MC	SCN11	0.918	0.932	−1.01	2.42
	SCN12	0.919	0.934	−0.961	2.403
	SCN13	0.92	0.935	−0.913	2.387
	SCN14	0.922	0.937	−0.866	2.372
	SCN15	0.927	0.945	−0.588	2.28
	SCN16	0.931	0.957	−0.153	2.156
	SCN17	0.922	0.972	0.637	2.052
CLEVER	SCN11	0.473	0.727	1.053	4.778
	SCN12	0.521	0.740	1.314	4.635
	SCN13	0.575	0.745	2.075	4.489
	SCN14	0.575	0.742	2.252	4.502
	SCN15	0.630	0.783	1.690	4.236
	SCN16	0.678	0.824	1.045	3.828
	SCN17	0.668	0.848	0.452	4.079

Note: N/S = no solution.

for open-channel routing for the wide-tooth-comb-wave hydrographs that adopt a temporal increment of 5 min or shorter.

Conclusions

From the preceding description and analysis, it can be concluded that (1) all five kinematic wave schemes, the Chow linear, HEC, KINEROS, MC, and CLEVER, are applicable to open-channel routing for wide-tooth-comb-wave hydrographs observed in the highly regulated Peace River if the temporal and spatial increments are set properly, even though the longitudinal slope of the river and time of rise of the simulated hydrograph do not fulfill the conditions set by the previously published literature; (2) smaller temporal and spatial increments do not necessarily mean higher simulation accuracy for all five kinematic wave schemes; (3) the Chow linear scheme has the largest numerical dispersion among the five schemes; (4) the CLEVER scheme has smaller numerical dispersion than the Chow linear scheme; and (5) no large errors are present in the CLEVER scheme for any sizes of spatial increment because this scheme is a TVD scheme. Therefore, the CLEVER scheme is more appropriate than the other four schemes for kinematic wave open-channel routing for the wide-tooth-comb-wave hydrographs observed in the highly regulated Peace River, allowing modelers to use larger temporal and spatial increments so that the scheme is time efficient for real-time flood forecasting in British Columbia while relatively high accuracy can still be achieved. However, due to CLEVER's limitations, it is not recommended to apply the CLEVER scheme to the open-channel routing for the wide-tooth-comb-wave hydrographs with a temporal increment of 5 min or shorter.

Data Availability Statement

Some or all data, models, or codes used during the study were provided by a third party. Direct requests for these materials may be made to the providers as indicated in the Acknowledgments.

Acknowledgments

The author thanks all staff members of the BC River Forecast Centre for their support for this study in all aspects. All discharge data were downloaded from WSC's real-time hydrometric data website; codes for the Chow linear, HEC, KINEROS, and MC schemes used in this study were programed based on the relevant references listed in this article; the CLEVER model was used internally by the BC River Forecast Centre only, but the related codes used in this study can be programed based on the equations given in this study.

References

Chakravarthy, S., and S. Osher. 1983. "High resolution applications of the Osher upwind scheme for the Euler equations." In *Proc., AIAA 6th CFD Conf. 1983*. Reston, VA: American Institute of Aeronautics and Astronautics.

Chow, V. T., D. R. Maidment, and L. W. Mays. 1988. *Applied hydrology*. New York: McGraw-Hill.

Dawdy, D. R. 1990. "Discussion of 'Kinematic wave routing and computational error' by T. V. Hromadka II and J. J. DeVries (February, 1988, Vol. 114, No. 2)." *J. Hydraul. Eng.* 116 (2): 278–280. https://doi.org/10.1061/(ASCE)0733-9429(1990)116:2(278).

Foster, H. D. 2001. "Landforms and natural hazards. "Chap. 3 in *British Columbia, the Pacific province: Geographical essays*, edited by C. J. B. Wood, 27–44. Victoria, BC, Canada: Univ. of Victoria.

Fread, D. L. 1993. "Flow routing." Chap. 10 in *Handbook of hydrology*, edited by D. R. Maidment, 10.1–10.36. New York: McGraw-Hill.

Godunov, S. K. 1959. "A difference method for numerical calculation of discontinuous solutions of the equations of hydrodynamics." [In Russian.] *Mat. Sb., N. Ser.* 47 (89): 271–306.

Lee, K. T., and P. C. Huang. 2012. "Evaluating the adequateness of kinematic-wave routing for flood forecasting in midstream channel reaches of Taiwan." *J. Hydroinf.* 14 (4): 1075–1088. https://doi.org/10.2166/hydro.2012.093.

Lettenmaier, D. P., and E. F. Wood. 1993. "Hydrologic forecasting." In *Handbook of hydrology*, edited by D. R. Maidment. New York: McGraw-Hill.

Lien, F. S., and M. A. Leschziner. 1994. "Upstream monotonic interpolation for scalar transport with application to complex turbulent flows." *Int. J. Numer. Methods Fluids* 19 (6): 527–548. https://doi.org/10.1002/fld.1650190606.

Luo, C. 2015. *Technical reference for the CLEVER model—A real-time flood forecasting model for British Columbia*. Victoria, BC, Canada: River Forecast Centre.

Luo, C., T. Gardner, and D. Campbell. 2015. "Evaluation of the CLEVER model—A real-time flood forecast model for large-scale watersheds in British Columbia." In *Proc., CWRA BC Branch Conf.* Vancouver, BC, Canada: Canadian Water Resources Association.

Luo, Q. 2007. "A distributed surface flow model for watersheds with large water bodies and channel loops." *J. Hydrol.* 337 (1–2): 172–186. https://doi.org/10.1016/j.jhydrol.2007.01.029.

Nash, J. E., and J. V. Sutcliffe. 1970. "River flow forecasting through conceptual models, 1. A discussion of principles." *J. Hydrol.* 10 (1): 282–290. https://doi.org/10.1016/0022-1694(70)90255-6.

Patankar, S. V., and D. B. Spalding. 1972. "A calculation procedure for heat, mass and momentum transfer in three-dimensional parabolic flows." *Int. J. Heat Mass Transfer* 15 (10): 1787–1806. https://doi.org/10.1016/0017-9310(72)90054-3.

Phillips, J. V., and S. Tadayon. 2007. *Selection of manning's roughness coefficient for natural and constructed vegetated and non-vegetated channels, and vegetation maintenance plan guidelines for vegetated channels in central Arizona*. Washington, DC: USGS.

Ponce, V. M. 1996. "Modeling surface runoff with kinematic, diffusion, and dynamic waves." In *Proc., Int. Conf. Hydrology and Water Resources*, 121–132. Berlin: Springer.

Preissmann, A. 1961. "Propagation des intumescences dans les canaux et Rivieres." In *Proc., First Congr. des l'Assoc. Francaise de Calcul*, 433–442. Grenoble, France: Association Francaise de Calcul.

Roe, P. L. 1981. "Approximate Riemann solvers, parameter vectors, and difference schemes." *J. Comp. Phys.* 43 (81): 357–372. https://doi.org/10.1016/0021-9991(81)90128-5.

Roe, P. L. 1986. "Characteristic-based schemes for the Euler equations." *Ann. Rev. Fluid Mech.* 18 (1): 337–365. https://doi.org/10.1146/annurev.fl.18.010186.002005.

Smith, R. E., D. C. Goodrich, D. A. Woolhiser, and C. L. Unkrich. 2012. "KINEROS—A KINematic runoff and EROSion model." Chap. 20 in *Computer models of watershed hydrology*, edited by V. P. Singh, 697–732. Washington, DC: Water Resources Publications.

Sweby, P. K. 1984. "High resolution schemes using flux limiters for hyperbolic conservation laws." *SIAM J. Numer. Anal.* 21 (5): 995–1011. https://doi.org/10.1137/0721062.

Todini, E. 2007. "A mass conservative and water storage consistent variable parameter Muskingum-Cunge approach." *Hydrol. Earth Syst. Sci.* 11 (1): 1645–1659. https://doi.org/10.5194/hess-11-1645-2007.

Tsai, C. W. 2003. "Applicability of kinematic, noninertia, and quasi-steady dynamic wave models to unsteady flow routing." *J. Hydraul. Eng.* 129 (8): 613–627. https://doi.org/10.1061/(ASCE)0733-9429(2003)129:8(613).

USACE. 1993. "Introduction and application of kinematic wave routing techniques using HEC-1, TD-10." Accessed March 4, 2019. http://www.hec.usace.army.mil/publications/TrainingDocuments/TD-10.pdf.

USACE. 2000. "Hydrologic modeling system HEC-HMS, technical reference manual, March 2000, CPD-74B." Accessed March 4, 2019. http://www.hec.usace.army.mil/software/hec-hms/documentation/HEC-HMS_Technical%20Reference%20Manual_(CPD-74B).pdf.

Van Albada, G. D., B. Van Leer, and W. W. Roberts. 1982. "A comparative study of computational methods in cosmic gas dynamics." *Astron. Astrophys.* 108 (1): 76–84.

Van Leer, B. 1974. "Towards the ultimate conservative difference scheme, 11. Monotonicity and conservation combined in a second order scheme." *J. Comp. Phys.* 14 (4): 361–370. https://doi.org/10.1016/0021-9991(74)90019-9.

Van Leer, B. 1977. "Towards the ultimate conservative difference scheme III. Upstream-centered finite difference schemes for ideal compressible flow." *J. Comp. Phys.* 23 (3): 263–275. https://doi.org/10.1016/0021-9991(77)90094-8.

Waterson, N. P., and H. Deconinck. 1995. "A unified approach to the design and application of bounded higher-order convection schemes." In *Proc., 9th Int. Conf. on Numerical Methods in Laminar and Turbulent Flow*. Swansea, UK: Pineridge Press.